e.g., in a section cut parallel to plane 2 at one end of a *T* cylinder (321) compressed 20 per cent. In the central part of the section, the grains are more cloudy and have more densely spaced lamellae than those at the top and side of the section. The state of preferred orientation of *c* axis, as described later, confirms the obvious inference that strain has proceeded further in the central part of the cylinder than near the margin (especially the end margin). Measurement of average grain diameter in the direction normal to the foliation plane (3) in specimen 321 failed to show any consistent difference in grain size between more and less deformed sectors.

Petrofabric Analysis

Procedure.—Much the same procedure has been followed as for marble deformed at room temperature (Part III, p. 888–890). Measurements were made on 100 grains in a section cut parallel to *T* (*i.e.*, normal to the foliation) in all cases except *T* cylinders (306 and 321) deformed in compression. In these latter, sections cut parallel to plane 2 (also normal to the foliation) were used, and the measured poles were subsequently rotated into plane *T*. This modified procedure allowed more precise measurement of directions (especially *c* axes) which, as a result of deformation, had become aligned subparallel to the axis of applied stress —*i.e.*, at high angles to plane *T*. In every case it was possible to locate *c* axes, and all three $\{01\bar{1}2\}$ lamellae in more than 95 per cent of the grains on the measured traverse; so that corresponding orientation diagrams need not be corrected for the existence of a central "blind spot."

The *c* axis was located optically in all grains except certain highly twinned crystals in cylinders 252, 306, and 321, whose orientation favored $\{01\bar{1}2\}$ twinning. All visible $\{01\bar{1}2\}$ lamellae and $\{10\bar{1}1\}$ cleavages were measured in each grain and were identified by their mutual angular and zonal relationships. The same data were used to check the optically determined positions of the *c* axes, or to locate these where optical determination was impossible. There is a general tendency, noted also in marble deformed at room temperature, for the angle between *c* and the pole of $\{01\bar{1}2\}$ to exceed somewhat the theoretical value of $26\frac{1}{4}°$. We offer no explanation for this effect, which must be connected with deformation since we have observed nothing comparable in undeformed Yule marble.

Orientation diagrams have been constructed for three crystal directions:

(1) The *c* crystal axis.

(2) Poles of most strongly developed $\{01\bar{1}2\}$ lamellae. One such is clearly recognizable in most grains. Where two sets are about equally strong in a given grain, both are plotted.

(3) Edges $[e:e]$ between the two strongest sets of lamellae in each grain. In the majority of grains one set (e_1) is well developed, a second set (e_2) somewhat less so, and the third set (e_3) is inconspicuous or lacking.

Axes a_1, a_2, a_3 were plotted in two cases (176, 321) but yielded no consistently recognizable pattern. Spacing indices for individual sets of $\{01\bar{1}2\}$ lamellae were not determined in this series of fabric analyses.

Preferred orientation of optic axis c.—In the undeformed marble fabric the *c* axes of calcite grains tend to lie at high angles to the plane of foliation (faces 1 and 3). In corresponding orientation diagrams (Fig. 6) there is a distinct but somewhat dispersed maximum around the pole of faces 1 and 3. This pattern may still be recognized as an element in the fabrics of deformed marbles even where the strain is of the order of 20 per cent. It is most persistent in the fabric of cylinders whose orientation in relation to applied stress precludes twin gliding in the majority of grains (Fig. 7, B, C). Such behavior accords completely with predictions based on the hypothesis of homogeneous deformation put forward by Handin and Griggs (Part II).

Compression at right angles to the foliation (255; Fig. 7, B) and extension parallel to it (176; Fig. 7, C) sharpen the original concentration of *c* axes. In both cases, *c* axes have been eliminated (presumably by nearly complete twinning) from the central part of the diagram.[1]

[1] From a statistical standpoint this is only a minor feature of the fabric, subject to over or underemphasis in a fabric analysis based on as few as 100 measurements. We have therefore verified the nonexistence of *c* axes in the central areas of Figures 7,B and 7,C by rapid traverses of several hundred grains in sections cut parallel to *T* (the plane of projection).

In Figure 7, B the maximum which coincides with the direction of shortening is strong and sharply defined compared with the narrowed but more extended maximum of Figure 7, C. The latter has been drawn out into an incomplete girdle in the plane normal to the axis of extension of the specimen. Note, too, how the few *c* axes initially subparallel to the foliation but normal to the axis of extension survive unchanged at the north and south poles of Figure 7, C, thus emphasizing further the partial girdle pattern of this diagram. No such *c* axes survive in Figure 7, B, for in this case corresponding grains were favorably oriented for twinning on $\{01\bar{1}2\}$.

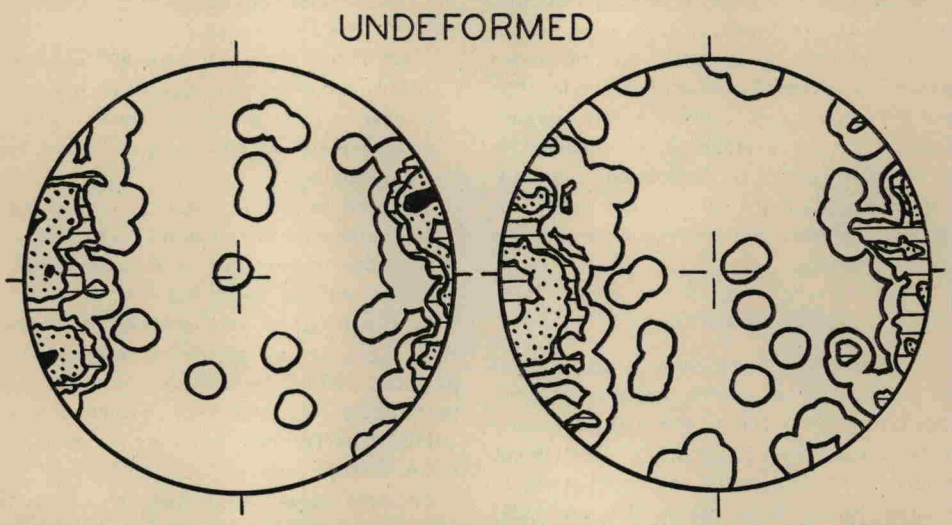

FIGURE 6.—ORIENTATION DIAGRAMS FOR *c* AXES OF CALCITE IN UNDEFORMED YULE MARBLE
100 grains per diagram. Contours, 1, 3, 5, 10%, per 1% area. The pole of the *B* surface of the block is at the center (lower hemisphere). Foliation is normal to plane of diagrams, parallel to N-S diameters.

Figures 7, A (321; compression parallel to foliation) and 7, D (252; elongation normal to foliation) are orientation diagrams constructed for specimens in which the majority of grains are strongly twinned on one or more $\{01\bar{1}2\}$ planes. In many such grains there is a choice between two alternative positions of *c* axes, one in the original lattice, the other in the lattice newly developed by twinning on $\{01\bar{1}2\}$. The *c* axis of that lattice which occupies the greater aggregate area within a given grain has been plotted in each case. There are a few grains where the initial and the twinned lattice are about equally developed; and here both *c* axes have been plotted. In both diagrams the initial pattern, though not destroyed, is in process of being obliterated. In Figure 7, A a new central concentration of *c* axes is developing. Note that this is parallel to the axis of compression, indicating not only that corresponding grains have been twinned to a high degree but that they have been rotated through angles of the order of 10° to 30°, so that their *c* axes approach the axis of compression. The pattern of Figure 7, D is distinctly weaker, since stress conditions in this case have dispersed *c* axes of twinned lattices through a broad vertical zone wherein they lie at high angles to the axis of extension.

Figure 7, E shows the orientation pattern resulting from extension in a direction inclined at 45° to the foliation. The initial concentration of *c* axes, though still recognizable, has been skewed away from the axis of extension, perpendicular to which a girdle of *c* axes is in process of formation. Twinning on $\{01\bar{1}2\}$ is the only glide mechanism powerful enough to eliminate the majority of *c* axes from the top right and lower left quadrants of the diagram. Its effectiveness is confirmed by plotting separately the two possible positions of *c* axes for each of a number of grains (18 per cent of those measured) in which twinning is so obvious that there are two alternative *c* directions. Such are interpreted as crystals whose